

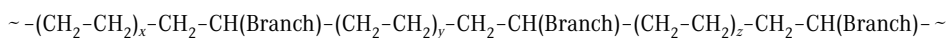
# 1

## Educational Minimum: Synthesis, Structure, and Properties of Polyethylene Resins

### ■ 1.1 Classification and Applications of Polyethylene Resins

The term “polyethylene resins” describes catalytically produced semi-crystalline homopolymers and copolymers derived mostly from ethylene [1-4], as well as ethylene polymers produced in radical polymerization reactions under high pressure [4-6]. Polyethylene resins of different types are widely used as commodity plastics.

Some polyethylene resins contain strictly linear polymer chains; their chemical formula is  $-(\text{CH}_2-\text{CH}_2)_n-$ , where  $n$  is a very large number, from  $\sim 1,000$  to  $\sim 100,000$ . Other polyethylene resins contain branches in their chains. Most such resins are produced in ethylene/ $\alpha$ -olefin copolymerization reactions. The molecular structure of ethylene/ $\alpha$ -olefin copolymers with a low  $\alpha$ -olefin content can be approximately represented by the formula:



where the  $-\text{CH}_2-\text{CH}_2-$  units come from ethylene and the  $-\text{CH}_2-\text{CH}(\text{Branch})-$  units come from the  $\alpha$ -olefin molecule. The  $x$ ,  $y$ , and  $z$  values in these chains can vary from small (4 to 5) to a very large number.

All the branches in catalytically produced polyethylene resins are of the same size; they are the alkyl substituents in the  $\alpha$ -olefin molecules: the ethyl group if the  $\alpha$ -olefin is 1-butene, the butyl group if the  $\alpha$ -olefin is 1-hexene, the hexyl group if the  $\alpha$ -olefin is 1-octene, or the isobutyl group if the  $\alpha$ -olefin is 4-methyl-1-pentene. When ethylene is polymerized at a high pressure via the radical mechanism, they have essentially the same chain structure. In this case, branches of several different types are formed spontaneously due to peculiarities of the radical polymerization reactions. These branches are linear or branched alkyl groups [7, 8]. Their lengths vary widely within each polymer molecule. Two types of such branches are distinguished: short-chain branches, from the methyl to the isoctyl group, and

**Table 1.1** Commercial Classification of Polyethylene Resins

Resin type	Symbol	$\alpha$ -Olefin content, mol %	Crystallinity degree, %	Density, g/cm <sup>3</sup>
Resins of high density	HDPE	0	65 to 70	>0.960
Resins of high density	HDPE	0.2 to 0.5	60 to 65	0.941 to 0.959
Resins of ultrahigh molecular weight	UHMW HDPE	0	30 to 40	0.930 to 0.935
Resins of medium density	MDPE	1 to 2	45 to 55	0.926 to 0.940
Resins of low density	LLDPE	2.5 to 3.5	30 to 45	0.915 to 0.925
Resins of very low density	VLDPE	>4	<25	<0.915
Low density polyethylene produced in radical reactions	LDPE	Branching degree 20 to 30 CH <sub>3</sub> /1,000C	45 to 55	0.910 to 0.940

The content of an  $\alpha$ -olefin in commercially manufactured ethylene/ $\alpha$ -olefin copolymers varies in a wide range, from <0.5 up to 20 mol %. These copolymers, depending on the content of  $\alpha$ -olefin, are called *medium density polyethylene resins* (MDPE), *linear low density polyethylene resins* (LLDPE), or *very low density polyethylene resins* (VLDPE). The group of the VLDPE resins is further divided into two subgroups, polyethylene *plastomers* with a crystallinity degree of 10 to 20% and density from 0.915 to 0.900 g/cm<sup>3</sup>, and completely amorphous ethylene *elastomers* with density as low as 0.86 g/cm<sup>3</sup>. By definition, all the catalytically produced resins contain only short-chain branches derived from  $\alpha$ -olefins. However, polymerization reactions utilizing some metallocene catalysts and chromium oxide catalysts can also introduce long-chain branches in the polyethylene chains (Section 1.4).

Some metallocene catalysts can copolymerize ethylene with cycloolefins, such as cyclopentene, cyclooctene, or norbornene. In this case, the branches in polyethylene chains are either small cycles containing from 5 to 10 carbon atoms, or two fused cycles. These materials form an additional resin type called *cycloolefin copolymers* (COC).

The five categories of polyethylene resins are specified according to their melt index measured according to ASTM D1238-10:

Category:	1	2	3	4	5
Melt index, g/10 min:	>25	10 to 25	1 to 10	0.4 to 1.0	below 0.4

Other characteristics of polyethylene resins, predominantly color, are specified by class. The three classes of polyethylene resins are designated as A, B, and C. The classes indicate color, amounts, and types of antioxidants, and other additives.

Class A refers to naturally colored polyethylene resins, Class B includes white and black-colored resins, and Class C covers weather-resistant black resins containing more than 2% carbon black.

The classification of polyethylene resins in its present form affords a basic distinction between different resin types. However, the classification is often poorly suited to delineate fine differences between structures and properties of various resins that play an important role in the sophisticated modern resin market. After all, the market grades different resins mostly according to their end-use properties rather than by their general classification.

Taken together, polyethylene resins account for the largest fraction, ~35%, of the worldwide plastic production. The volume of HDPE resins manufactured worldwide in 2019 was over 50 million metric tons and the combined volume of LLDPE and LDPE resins over 60 million metric tons. In the US alone, the total production volume of all polyethylene grades in 2019 amounted to ~23 million metric tons.

Applications of polyethylene resins vary greatly by the grade. The applications of the two most important grades are:

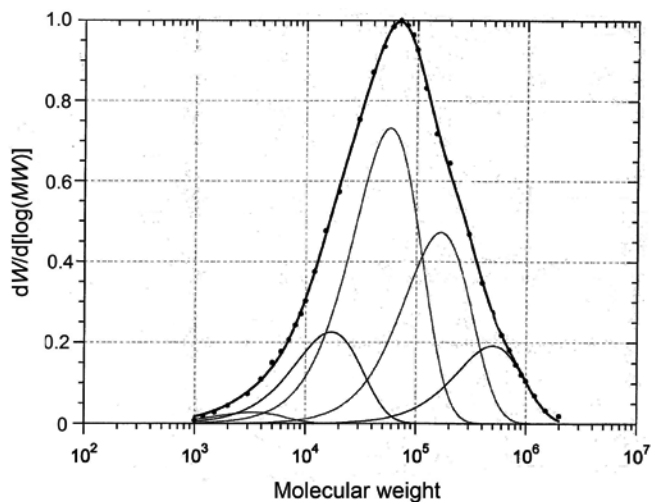
HDPE resins	Blow molding (containers and bottles)	~31%
	Film (biaxially oriented)	~28%
	Injection molding	~22%
	Other applications	~19%
LLDPE resins	Film (blown and cast)	~80%
	Injection molding	~7%
	Wire and cable coating/insulation	~4%
	Other applications	~9%

## ■ 1.2 Catalysts for Synthesis of Polyethylene Resins

Polyethylene resins are produced commercially with transition metal catalysts of different types [1–4, 9, 10] or in high-pressure radical polymerization reactions [4, 5]. This section provides merely a brief sketch of the catalyst chemistry; a much more detailed discussion of catalyst preparation techniques is presented in reviews [3, 4, 9, 10].

Several groups of polymerization catalysts are especially important.

*Titanium-based Ziegler-Natta catalysts:* All these catalysts consist of two components. The first component is called a *catalyst*, it is a liquid or a solid powder that



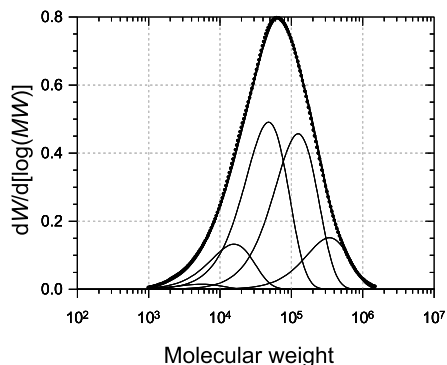
**Figure 1.5** Experimental GPC curve of HDPE resin produced with supported Ziegler-Natta catalyst at 80 °C (points) and its resolution into Flory components

Table 1.2 gives parameters  $M_w$  and  $FR_j$  of each Flory component in this resin. The numbering of Flory components used in the table, from I to IV in the order of increasing molecular weight, as well as numbering of Flory components in all the following tables, is arbitrary.

**Table 1.2** Flory Components in HDPE Resin Produced with Supported Ziegler-Natta Catalyst

Flory component (j)	Molecular weight ( $M_{w,j}$ )	Content ( $FR_j$ ), %
I	15,700	14
II	47,900	45
III	124,400	29
IV	342,900	12
Total resin	133,000	100

Figure 1.6 shows the GPC curve of an LLDPE resin (ethylene/1-hexene copolymer with  $C_M^{\text{copol}} = 3.5$  mol) produced with a supported Ziegler-Natta catalyst at 85 °C. The product is also a mixture of four Flory components [49]. The distribution of copolymer molecules with respect to their molecular weight in these LLDPE resins is also quite broad, similarly to HDPE resins produced with catalysts of the same type (Figure 1.5) [42, 50]. The width of the molecular weight distribution  $(M_w/M_n)^{\text{av}}$  of the copolymer is 4.0.

**Figure 1.6**

Experimental GPC curve of LLDPE resin (ethylene/1-hexene copolymer with  $C_M^{\text{copol}} = 3.5$  mol %) produced with supported Ziegler-Natta catalyst and its resolution into Flory components

Table 1.3 gives parameters of each Flory component in the copolymer mixture. Detailed kinetic analysis of ethylene/1-hexene copolymerization reactions with supported Ziegler-Natta catalysts showed [50–52] that Flory components in the copolymers differ not only in the average molecular weight but also in the 1-hexene content. As Table 1.3 shows, the components with the lowest molecular weight (components I and II) have the highest 1-hexene content whereas the components with the highest molecular weight (components III and IV) have the lowest 1-hexene content. The existence of the differences in the copolymer composition was confirmed with several crystallization fractionation studies described in Section 1.8 (see Table 1.7).

**Table 1.3** Flory Components in LLDPE Resin Produced with Supported Ziegler-Natta Catalyst

Flory component (j)	Molecular weight ( $M_{w,j}$ )	Content ( $FR_j$ ), %	$C_M^{\text{copol}}$ , mol %
I	15,700	11	8 to 10
II	47,900	39	~4
III	124,400	37	0.6 to 0.8
IV	342,900	12	0.3 to 0.4
Total resin	109,000	100	3.5

### 1.6.3 Polyethylene Resins Produced with Chromium Oxide Catalysts

Figure 1.7 shows the GPC curve of a typical HDPE resin prepared with a chromium oxide catalyst. The molecular weight distribution of such resins is always very broad; seven Flory components are needed to represent this GPC curve. Table 1.4 lists molecular weights of Flory components in an HDPE resin produced at 90 °C.

# 2

## Melt Index and Melt Flow Ratio of Polyethylene Resin

### ■ 2.1 Introduction

The melt index of a polyethylene resin is universally accepted in the industry as an indicator of the resin's average molecular weight. Melt indexes are routinely measured both in the industrial environment and in laboratory using simple automated equipment and simple standard procedures (Section 2.1.1). The polymer science operates with a different set of parameters describing molecular weight characteristics of ethylene polymers. The three most often used parameters are the weight-average molecular weight  $M_w$ , the number-average molecular weight  $M_n$ , and the width of the molecular weight distribution, the  $M_w/M_n$  ratio. Measurement methods and the statistical meaning of these parameters are described in Section 1.5 of Chapter 1.

This chapter describes correlations between these two sets of molecular weight characteristics.

#### 2.1.1 Measurement Method of Melt Index

Melt indexes of polyethylene resins are measured using the instrument called an *extrusion plastometer*. The measurement procedures are specified in the American Society for Testing and Materials (ASTM) method D1238-10, Conditions E and F, and in the International Organization for Standardization (ISO) Method 1133. Figure 2.1(a) shows the schematics of the melt index measurement. A small amount of resin (~6 gram) is placed inside the heated cylindrical barrel (9.55 mm diameter) with a metal die at its bottom. The die has a round capillary opening, 2.095 mm in diameter and 8 mm in length. Some procedures use a shorter die (a half-die) 4 mm long with a 1.0475 mm capillary opening. A metal plunger with a long narrow stem is placed on the top of the resin sample. The resin is kept at 190 °C for 6 minutes to achieve complete melting. After that, the melt is pressurized by placing a cylindrical metal weight on the upper tip of the stem. The pressure of the plunger

forces the melt through the capillary opening. By definition, the melt index of a polyethylene resin is the weight of the melt extruded through the capillary over a period of 10 minutes, that is, the melt index is a measure of the melt flow rate (g/10 min). Depending on the type of polyethylene resin, four different standard weights (the total of the cylindrical metal weight, the plunger, and the rod) are used to measure melt indexes, 2.16, 5.16, 10.16, and 21.6 kg. The melt indexes are respectively designated as  $I_2$ ,  $I_5$ ,  $I_{10}$ , and  $I_{21}$ . If no indication of the weight is given, the  $I_2$  value is traditionally reported. In the earlier designs of extrusion plastometers, the polymer extrudate was collected, cooled, and its amount was determined by weighing. Modern extrusion plastometers use an automated procedure; they measure the speed of the downward movement of the plunger under a given weight.

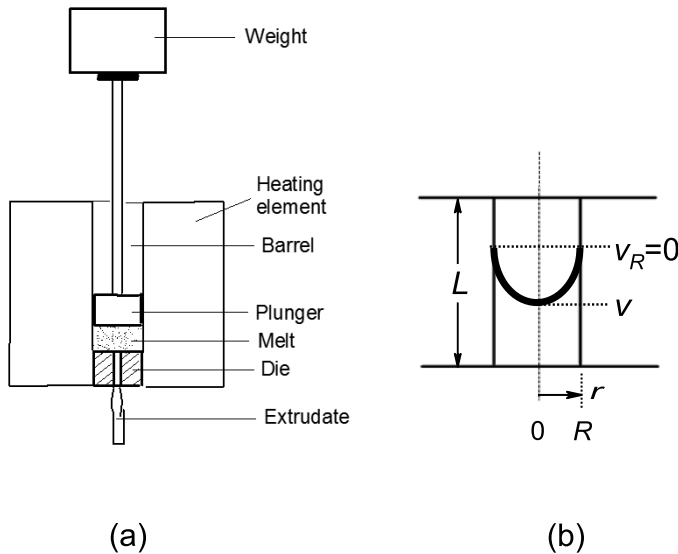


**Figure 2.1** (a) Schematics of melt index measurement; (b) flow of viscous liquid through capillary

### 2.1.2 Empirical Correlations between Melt Index and Molecular Weight

If one is dealing with polyethylene resins of a single particular type (for example, resins produced with the same catalyst under different reactor conditions), the melt index is a precise relative measure of the resin's weight-average molecular weight  $M_w$ . Several empirical correlations between  $M_w$  values and melt indexes of various polyethylene resins were developed. Figure 2.2 shows one such example

## ■ 3.3 DSC Melting Curves and Melting Points of LLDPE and VLDPE Resins Produced with Single-Site Catalysts

### 3.3.1 Effect of Crystallization Conditions

Compositionally uniform ethylene/ $\alpha$ -olefin copolymers prepared with single-site metallocene catalysts represent a convenient model to examine the effect of crystallization conditions on the shape of DSC melting curves. Figure 3.3 demonstrates this effect using as an example two ethylene/1-hexene copolymers prepared with different metallocene catalysts in toluene slurry at 70 °C [25]. The copolymers have a different composition: the sample in Figure 3.3(A) contains 0.8 mol % of 1-hexene and the sample in Figure 3.3(B) 2.4 mol %. Their crystallinity degree is also different, 63% and 42%, respectively. Ethylene copolymerization reactions in toluene slurry are accompanied by orderly crystallization of polymer molecules. DSC peaks of both nascent copolymers (materials recovered from polymerization reactors without any additional thermal treatment) are relatively narrow (Figure 3.3(A) and Figure 3.3(B)). When the mixture of the two copolymers is slowly crystallized from toluene solution, each component forms separate crystals (Figure 3.3(C)).

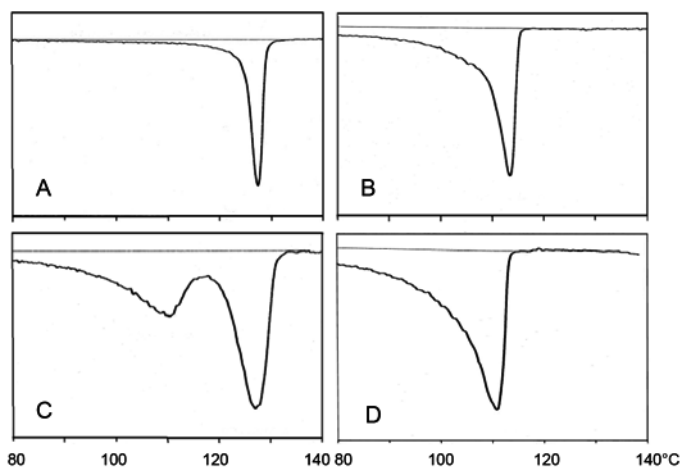


**Figure 3.3** DSC melting curves in the narrow temperature range 80 – 140 °C: A and B – nascent copolymers with  $C_M^{\text{copol}} = 0.8$  and 2.4 mol %, respectively, produced with two metallocene catalysts; C – mixture of the two copolymers crystallized from solution; D – re-melted copolymer B



When these compositionally uniform copolymers are crystallized from the melt, the lamella-formation process is much faster and less orderly than during crystallization from solution or during a polymerization reaction. The DSC peak of a thermally pretreated copolymer (Figure 3.3(D)) is broader than the DSC peak of the solution-crystallized copolymer (Figure 3.3(B)), and its melting peak is positioned at a lower temperature. This comparison emphasized the need for a thoroughly followed protocol in the preparation of resin samples for the DSC analysis. Analytical laboratories often examine polymer samples with unknown or poorly defined thermal history. A standardized procedure, for example, pre-melting of a resin specimen in a hot press, is a desired step for a DSC sample preparation.

### 3.3.2 Effect of Copolymer Composition

Figure 3.4 shows melting points of compositionally uniform ethylene/1-hexene copolymers produced with single-site metallocene catalysts as a function of their composition. The copolymers contain from 0.5 to 3.5 mol % of 1-hexene. All the materials were thoroughly homogenized before the DSC analysis by hot-pressing polymer powders into thick film. The melting points were measured during the second melting step; each corresponds to the maximum on the DSC melting curve. The results show that the melting point decreases with an increase in the 1-hexene content in the copolymers. This section describes a DSC model which provides an explanation for the steep dependence between  $T_m$  and  $C_M^{\text{copol}}$  values evident from Figure 3.4.

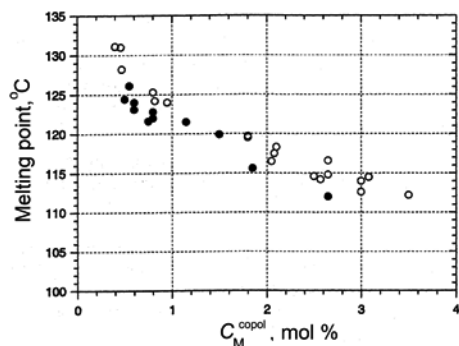


**Figure 3.4**

Melting temperatures of ethylene/1-hexene copolymers of different composition produced with single-site metallocene catalyst; heating rates are 10 °C/min (●) and 2 °C/min (○)

Basic statistical expressions used for modeling the melting behavior of compositionally uniform ethylene/ $\alpha$ -olefin copolymers are given in Section 1.7 of Chapter 1. For the goal of the DSC modeling, a copolymer chain can be viewed as consisting of a set of monomer sequences; blocks of ethylene units,  $M-(E)_n-M$ , and blocks of  $\alpha$ -olefin units,  $E-(M)_m-E$ . All commercial LLDPE and VLDPE resins contain rela-

curve are the yield point, the end-of-necking point, and the breaking point. These points are characterized by six parameters:

1. The yield stress,  $\sigma_y$ , and the yield strain,  $\varepsilon_y$ ;
2. The necking stress,  $\sigma_n$ , and the end-of-necking strain,  $\varepsilon_n$ ;
3. The breaking (tensile) stress,  $\sigma_{br}$ , and the breaking strain,  $\varepsilon_{br}$ .

The  $\varepsilon$  values in Figure 1.18 are the length ratios in the strained and the original sample:  $\varepsilon = \text{elongation} + 1$ ; the minimum  $\varepsilon$  value for a polymer sample before stretching is 1.

Mechanical changes shown in Figure 1.18 are accompanied by irreversible structural changes in the polymers; they are schematically shown in Figure 1.19. After the yield point of a polymer sample is passed, an area consisting of a highly oriented material (the neck) develops in the strained sample. As the stretching proceeds further, the two principal morphological features of a semi-crystalline resin, the spherulites and the microfibrils (see Figure 1.16 and Figure 1.17), are gradually disassembled until all the material in the tested sample becomes highly oriented. This transformation occurs at a nearly constant necking stress  $\sigma_n$ . The last stage of the sample stretching is called strain hardening; it involves a simultaneous further increase in the strain and the stress in the oriented sample. At some point during this stage the material finally breaks. The length of the strain-hardening range,  $\varepsilon_{br} - \varepsilon_n$ , depends on the grade of the resin. HDPE resins break soon after the onset of strain hardening; their  $\sigma_y$  and  $\sigma_{br}$  values are relatively close. On the other hand, LLDPE resins have a relatively large strain-hardening range and their  $\sigma_{br}$  value is always much higher than the  $\sigma_y$  and the  $\sigma_n$  values.

Two more mechanical parameters are used to characterize polyethylene resins. The first parameter, the Young's modulus ( $M_{\text{Young}}$ ), characterizes stiffness of a resin sample, the slope of the stress/strain curve at very low strain. By definition,  $M_{\text{Young}} = d(\sigma)/d(\varepsilon - 1)$  at low  $\varepsilon$ . In practice, two similar parameters, the secant modulus, are often used, the stress at 1% elongation or at 2% elongation. The second mechanical parameter, the strain-hardening modulus ( $M_{\text{str-hard}}$ ), characterizes stiffness of a fully stretched and oriented resin sample:  $M_{\text{str-hard}} = (\sigma_{br} - \sigma_n)/(\varepsilon_{br} - \varepsilon_n)$ .

### 5.1.1 Effect of Stretching Speed on Mechanical Properties

Both end-use mechanical tests of polyethylene film, the dart impact test and the tear test, are carried out at a high deformation speed (Section 5.2 and Section 5.3). Relaxation phenomena in polyethylene are relatively slow, and most mechanical parameters of the resins depend on the deformation speed [8, 9]. These dependencies were measured experimentally in a broad range of deformation speeds  $V$  from 0.5 to 150 cm/min (0.2 to ~60 in/min) for several ethylene/1-hexene LLDPE res-

ins, both compositionally uniform resins produced with metallocene catalysts and compositionally nonuniform resins produced with Ziegler-Natta catalysts. In most cases, the dependencies between the tested parameters,  $\sigma$  or  $\varepsilon$ , and the deformation speed can be represented by simple empirical relationships using as a standard a particular  $\sigma$  or  $\varepsilon$  value at the standard deformation speed  $V_{\text{stand}}$  of 50.8 cm/min (20 in/min):

$$\sigma_y(V) = \sigma_y^{\text{stand}} + k(\sigma_y) \cdot \log(V/V_{\text{stand}}), \quad \text{the slope } k(\sigma_y) \approx 0.14 \quad (5.1)$$

$$\sigma_n(V) = \sigma_n^{\text{stand}} + k(\sigma_n) \cdot \log(V/V_{\text{stand}}), \quad \text{the slope } k(\sigma_n) \approx 0.11 \quad (5.2)$$

$$\varepsilon_n(V) - \varepsilon_y(V) = \varepsilon_n^{\text{stand}} - \varepsilon_y^{\text{stand}} + k(\varepsilon_n - \varepsilon_y) \cdot \log(V/V_{\text{stand}}) \quad (5.3)$$

The slope  $k(\varepsilon_n - \varepsilon_y)$  in the last expression varies from 0.5 to 0.6 depending on the LLDPE grade. Three other parameters of the stress/strain curve,  $\varepsilon_y$ ,  $\varepsilon_{br}$ , and  $\sigma_{br}$ , practically do not depend on the deformation speed.

### 5.1.2 Orientation in Polyethylene Film

Figure 5.1 shows the orientation pattern, orientation of the  $c$  axis in crystallites (the direction of molecular chains) in two types of articles manufactured from polyethylene, a blow-molded item and film.

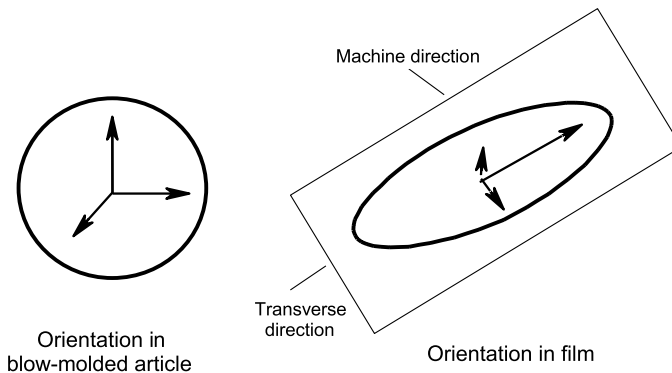


**Figure 5.1** Orientation distribution in blow-molded article and in film

Thick-walled, blow-molded articles are practically isotropic in terms of chain orientation. On the other hand, polymer chains in polyethylene film are preferably oriented in the machine direction of film manufacture. The level of orientation depends on the resin type; it is the highest in HDPE film but significantly lower in

## 6.4.5 Mechanism of Environmental Stress Cracking

The mechanism of the polyethylene failure under the environmental stress cracking conditions represents a special case of the general mechanism describing the mechanical failure of polymers under low stress, which is discussed in Section 6.3.2. Similar to the process of failure under low stress, the environmental stress cracking mechanism includes four distinct stages [59, 60]:

craze nucleation (the longest stage) → craze growth → craze failure (crack initiation) → crack propagation.

The overall behavior of polyethylene articles under the conditions of environmental stress cracking is similar to that of their failure under low stress. Both processes are dominated by the molecular entanglement network, which is formed in the polymer melt prior to crystallization [38] (Section 6.3.2). Crystallization of most polyethylene resins from the melt leads to a spontaneous fractionation of their components. The low molecular weight and branched macromolecules crystallize at the latest stage of crystallization and concentrate in interlamellar and inter-spherulite regions. These short polymer chains cannot serve as good ties between lamellae and between spherulites. The principal feature responsible for the ESCR is the presence of tie molecules of a high molecular weight, which reinforce mechanically weak areas between and within spherulites and mitigate the effects of polymer fractionation [18, 38, 45–49]. The content of tie molecules in an HDPE resin can be artificially increased, for example, by co-blending a small amount of a semi-crystalline ethylene block copolymer with the resin [61] or by co-blending an HDPE resin with a high molecular weight LLDPE resin, especially if the LLDPE resin contains a small amount of long-chain branches [62].

Two subjects are important for the discussion of the mechanism of environmental stress cracking: the role of the detergent and the role of the solvent for the detergent. A detailed analysis of the liquid environment and its effect on the ESCR of LDPE and HDPE resins showed several important effects [17, 27, 30, 41, 52, 60].

Figure 6.12 compares schematically the crack propagation phenomena in an HDPE resin in three different environments: air, water, and 10% water solution of Igepal CO-630 [27]. The dependence between the stress and the speed of crack propagation measured in the air test shows the complex fatigue behavior typical for HDPE resins in general (Section 6.3.2). The cracks start to grow at a certain finite stress level. Initially, even a small increase of the stress leads to a rapid increase of the crack propagation rate but the acceleration of the crack propagation becomes less pronounced at high stresses. The behavior of the same HDPE resin in the water environment is mostly the same as in air, that is, water is not an effective sensitizing agent. An introduction of the detergent changes several features of the dependence between the stress and the crack growth rate:

1. The minimum stress required for the crack to start growing decreases about twofold.
2. A new stage in the crack propagation process becomes apparent: when the stress reaches a certain level, the speed of the crack growth does not depend on the stress.
3. The environmental stress cracking phenomena manifest themselves at relatively low stresses. The specific effect of a detergent disappears in the high-stress range of the curve in Figure 6.12 but this range (the range of a very short time-to-failure) is of little concern under the real-life conditions.
4. A very large difference exists in the speed of crack propagation between solutions of Igepal CO-630 in different solvents (Figure 6.13).

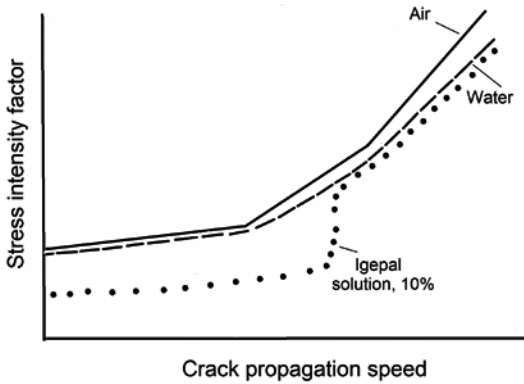


**Figure 6.12**

Crack propagation speed in HDPE sample in three environments; data from [30]

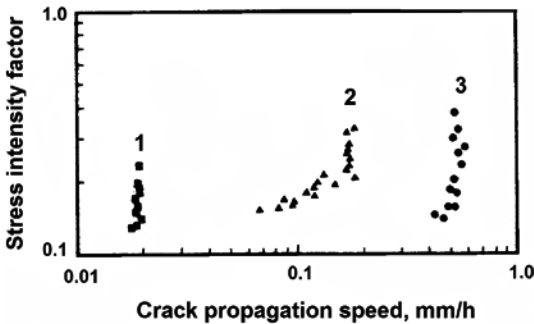


**Figure 6.13**

Environment effect on crack propagation speed in HDPE resin; data from [30]. Solvents for Igepal CO-630: (1) ethanol, (2) ethylene glycol, and (3) water

The ESCR of polyethylene resins strongly depends on the concentration of a detergent in water (Igepal CO-630 in this case) [63, 64]. The largest reduction in the time-to-failure occurs at a low detergent concentration of  $\leq 0.1\%$ . An additional increase of the detergent concentration up to  $\sim 20$  to  $25\%$  leads to a relatively small incremental reduction of the time-to-failure; the effect is minimal when the detergent concentration reaches  $50\%$ , and a further increase of the detergent concentration from  $50$  to  $100\%$  does not produce any effect at all.

# Index

## A

- Active center *9–11, 13*
- Additivity rules, for viscosity *53, 57*

## B

- Bimetallic catalysts *6, 22, 65*
- Bimodal resin *10, 22, 24*
- Bimodal resins *65*
- Blocks, in copolymers *25, 77, 93*
- Branches
  - long-chain *2, 13, 46, 68, 69*
  - short-chain *1*
- Branching degree *2*
- Breaking point, stress and strain *36, 102*
- Burst test, dynamic, for pipes and tubing *136*

## C

- Capillary, melt flow through *46*
- Catalysts, effects on resin properties
  - bimetallic *6, 23, 65*
  - chromium oxide *5, 7, 21, 22, 29*
  - metallocene *6, 8, 18, 31*
  - Ziegler-Natta *4, 6, 20, 21, 28, 62, 65*
- Chain orientation *103, 104, 128*
- Chain propagation reactions *10*
- Chain transfer (termination) reactions *11*
- Chromium-containing catalysts *5*
- Classification, of polyethylene resins *4*
- Compositional uniformity *27, 28*
- Copolymer chain statistics *25*
- Copolymerization reactions *12*

## CRYSTAF *27–30*

- Crystal forms of polyethylene *32, 95*
- Crystallinity degree
  - definition *93*
  - effect of copolymer composition *94*
  - measurement methods *91*

## D

- Dart impact strength of LLDPE film
  - definition *105*
  - measurement *105*
  - model *108, 110*
  - of ethylene copolymers *115*
- Density-gradient columns *95*
- Density of polyethylene resins
  - effect of copolymer composition *97*
  - measurement methods *95*
  - use in classification *2, 4*
- Differential scanning calorimetry (DSC)
  - *71, 91*
- Distribution of monomer units in copolymers *25*

## E

- Effective viscosity, additivity rules *53, 55*
- Environmental stress cracking resistance (ESCR)
  - definition *147, 152*
  - effect of density *150*
  - effect of molecular weight *148*
  - measurement methods *146*
  - mechanism *150, 152, 153, 156*

**F**

- Failure, low-stress 140, 142–144
- Flory-Schulz molecular weight distribution 16, 18

**G**

- Gas-phase polymerization technology 8
- Gel permeation chromatography (GPC) 15

**H**

- Haze 166
- Hazemeter 166
- Heat of fusion of polyethylene 92
- Hydrogen, chain transfer agent 11

**I**

- Infrared spectroscopy 32, 93, 104, 107

**L**

- Lamella 32, 33
- LLDPE film
  - blocking 164
  - end-use testing 159
- LLDPE resins
  - extractables and solubles 161
- Long-chain branching 2, 13, 46
- Low density polyethylene (LDPE) 3, 9
- Low-stress failure 140

**M**

- Melt flow rate 44, 50
- Melt flow ratio, definition 46
- Melt index 2, 44
  - definition 43, 44
  - of Newtonian liquid 50
  - of non-Newtonian liquid 51
  - of polyethylene resins 58, 64, 66, 68
  - polyethylene resins 46, 59

Melt Index 43

Melting curve, model

- HDPE 72–74
  - LLDPE 76, 77, 79, 81–83
- Melting points
- of ethylene copolymers 77
  - of linear polyethylene (HDPE) 72–74

Metallocene catalysts 6, 18, 19

- GPC analysis 18

Methylalumoxane (MAO) 6

Modeling

- dart impact test 107–109
- Elmendorf tear test 123, 124, 126
- top load test 136

Modelling

- Elmendorf tear test 122

Molecular weight distributions

- GPC analysis 16
- theory 14

Molecular weights of polyethylene resins 12, 13

- control with hydrogen 11
- measurement methods 15

Monodisperse polyethylene 45, 51, 52

Morphology, of polyethylene resins 31

**N**

- Necking stage, stress and strain 36, 102
- Newtonian liquid 46, 50, 52
- Nomenclature, of polyethylene resins 3
- Non-Newtonian liquid 46, 48, 51, 55
- Nuclear magnetic resonance (NMR) 91

**O**

Orthorhombic cell 31, 96

**P**

- PEX 139
- Pipes, testing 140
- Plastomers 3, 83
- Polyethylene film
  - haze 166

Polyethylene resins  
– applications 4  
– bimodal 22, 65, 68  
– branching degree 2  
– classification 2, 4  
– compositionally nonuniform 30, 113–115  
– compositionally uniform 27, 28  
– definition 1  
– morphology 31  
– multi-Flory 17, 19, 21, 23, 57, 58  
– nomenclature 3  
– single-Flory 18, 59, 60  
Polymerization degree 15  
Polymerization rate 11  
Polymerization reactors  
– gas-phase 7, 8  
– slurry (particle-type) 7  
– solution 8, 9  
Polymorphism of polyethylene 32, 96  
Pseudo-monoclinic cell 32, 96

## R

Radical reactions  
– cross-linking 139  
– polymerization 7, 9

## S

Secant modulus 35, 139  
Shear strain, definition 49  
Shear stress, definition 49  
Slurry polymerization technology 7, 9  
Spherulite 33–35  
Statistics of copolymer chains 25  
Stress-strain curve 35

## T

Tear strength of LLDPE film  
– model 122, 124, 126, 127  
Top load test, for containers  
– measurement 135  
– model 137  
TREF 27, 28

## U

Uniformity, compositional 27, 30

## V

Viscosity  
– definition 49  
– effective 55  
– zero-shear 47

## X

X-ray spectroscopy 32, 91

## Y

Yield stress and strain 35, 102  
Young's modulus 35, 112, 137, 138

## Z

Zero-shear viscosity  
– additivity rules 53, 55  
– definition 47